

# Black Hole Solutions in String Theory with Gauss-Bonnet Curvature Correction

Kei-ichi Maeda,<sup>1,2,\*</sup> Nobuyoshi Ohta,<sup>3,†</sup> and Yukinori Sasagawa<sup>1,‡</sup><sup>1</sup> *Department of Physics, Waseda University, Shinjuku, Tokyo 169-8555, Japan*<sup>2</sup> *Advanced Research Institute for Science and Engineering, Waseda University, Shinjuku, Tokyo 169-8555, Japan*<sup>3</sup> *Department of Physics, Kinki University, Higashi-Osaka, Osaka 577-8502, Japan*

(Dated: October 23, 2018)

We present the black hole solutions and analyse their properties in the superstring effective field theory with the Gauss-Bonnet curvature correction terms. We find qualitative differences in our results from those obtained in the truncated model in the Einstein frame. The main difference in our model from the truncated one is that the existence of a turning point in the mass-area curve, the mass-entropy curve, and the mass-temperature curve in five and higher dimensions, where we expect a change of stability. We also find a mass gap in our model, where there is no black hole solution. In five dimensions, there exists a maximum black hole temperature and the temperature vanishes at the minimum mass, which is not found in the truncated model.

PACS numbers: 04.20.Cv, 04.50.-h, 04.60.Cf, 04.70.Dy.

## I. INTRODUCTION

A black hole always absorbs the ambient matter and the mass increases in time classically. However, if we take into account the quantum effect, a black hole will emit the Hawking radiation and evaporate away. It behaves as a thermal object. Of course, such a quantum effect can be ignored for astrophysical black holes. On the other hand, for microscopic black holes, the situation drastically changes. The black hole loses its mass by the radiation and may vanish. When the mass approaches the Planck mass, however, the semiclassical approach is no longer valid. To know what happens at the end of evaporation, i.e., to answer the questions such as “What is the final state of black hole?” or “Does a naked singularity appear?”, we may need to study it by quantum gravity.

One of the most promising candidates for the quantum theory of gravity is the string theory, which may also provide us a unified theory of fundamental interactions (the so-called “theory of everything”) [1]. String theory is, however, still in a developing stage and may not yet be able to treat strong gravitational phenomena such as a black hole directly. Hence we shall study black holes in the effective field theory including string quantum correction terms. The field theory limit of the string theories leads to a ten-dimensional supergravity theory at the lowest derivative level. In addition, it is known that quantum effect gives higher curvature correction terms. There are five string theories in ten dimensions, which are related with each other via dualities. The curvature correction terms depend on the type of string theory. In the heterotic string theory, the lowest corrections are described by the second-order curvature term, i.e., the so-called Gauss-Bonnet term [2]. On the other hand, in type II string theory, the fourth-order curvature terms appear as the lowest [3].

The Gauss-Bonnet term is known as the second-order Lovelock gravity. The Lovelock theory is a higher curvature generalization of Einstein gravity. Its field equations contain terms up to the second-order derivatives of the metric functions and the second-order derivative terms are linear [4, 5]. The  $n$ -th order of Lovelock gravity is constructed by the Euler den-

sity in the  $2n$  dimensional spacetime. Hence,  $n$ -th terms with  $n \leq [(D-1)/2]$  contribute to the field equations. The black hole solution in the theory with the Gauss-Bonnet term or with the Lovelock action has been analysed in the models in many works [6, 7].

A dilaton field also plays an important role in the string theory as a dynamical field. Hence dilatonic models have been studied intensively in the context of string theory. The black hole solution in such a dilatonic theory was studied in [8] and [9]. The black hole solution with the Riemann curvature squared correction term coupled to dilaton was first studied by the linear perturbation approach [10]. When the Gauss-Bonnet term couples to a dilaton, it contributes to the dynamical equations even in four dimensions. Full study of this case requires numerical evaluation, and has been made in [11–16].

In the string frame, the Einstein-Hilbert curvature term is also coupled to the dilaton field. So usually we perform a conformal transformation to find the Einstein frame, in which the Einstein-Hilbert curvature term does not couple to the dilaton field. When we study a black hole in the Einstein frame, only the Gauss-Bonnet term is taken into account as the quantum correction, but some additional terms appear through a conformal transformation compared with the string frame. It is not so obvious which frame is to be used in investigating solutions where strong gravitational effects become strong such as black holes. It is certainly natural to take the action in the string frame in string theory, and then it is important to check if the above additional terms make any difference in the results. In this paper, we analyse black hole solutions in the effective action in the Einstein frame equivalent to that in the string frame, and compare the results with those in the truncated effective action, i.e., the model only with the Gauss-Bonnet term as the correction. Black hole solutions in the four-dimensional string frame are examined in the context of black hole - string transition in [17].

This paper is organized as follows: In Sec. II, we present the effective action which we discuss in this paper, and perform a conformal transformation to obtain the description in the Einstein frame. We also define our truncated model. In Sec. III, we write down the basic equations for a spherically symmetric and static spacetime in the dilatonic Einstein-Gauss-Bonnet theory, and give the boundary condition for the regular black hole horizon. We transform the variables in the string frame to those in the Einstein frame in Sec. IV. In Sec. V, we introduce the thermodynamical variables. We then show our

\*Electronic address: maeda@waseda.jp

†Electronic address: ohtan@phys.kindai.ac.jp

‡Electronic address: yukinori@gravity.phys.waseda.ac.jp

numerical results in Sec. VI. In Sec. VII, we briefly summarize the truncated dilatonic Einstein-Gauss-Bonnet model. We present the basic equations and the boundary conditions on the black hole horizon. We compare our results in the dilatonic Einstein-Gauss-Bonnet theory with those in the truncated one in Sec. VIII. The concluding remarks are made in Sec. IX.

## II. EFFECTIVE ACTION AND ITS TRUNCATION IN THE EINSTEIN FRAME

In this paper, we focus on the Einstein-Gauss-Bonnet gravity coupled to a dilaton field. The effective action of the heterotic string theory in the string frame is given by

$$\mathcal{S}_S = \frac{1}{2\kappa_D^2} \int d^D \hat{x} \sqrt{-\hat{g}} e^{-2\hat{\phi}} \left( \hat{R} + 4(\hat{\nabla}\hat{\phi})^2 + \alpha_2 \hat{R}_{GB}^2 \right), \quad (2.1)$$

where  $\kappa_D^2$  is the  $D$ -dimensional gravitational constant,  $\hat{\phi}$  is a dilaton field,

$$\hat{R}_{GB}^2 = \hat{R}^2 - 4\hat{R}_{\mu\nu}\hat{R}^{\mu\nu} + \hat{R}_{\mu\nu\rho\sigma}\hat{R}^{\mu\nu\rho\sigma}, \quad (2.2)$$

is the Gauss-Bonnet curvature term, and  $\alpha_2 = \alpha'/8$  is its coupling constant.

In the string frame, the dilaton field couples to the Ricci scalar curvature nonminimally. Hence we perform a conformal transformation

$$g_{\mu\nu} = \exp[-2\gamma^2 \hat{\phi}] \hat{g}_{\mu\nu}, \quad (2.3)$$

where  $\gamma^2 = \frac{2}{D-2}$ , in order to find the Einstein-Hilbert action. The action in the Einstein frame is given by

$$\mathcal{S}_E = \frac{1}{2\kappa_D^2} \int d^D x \sqrt{-g} \left[ R - \frac{1}{2}(\nabla\phi)^2 + \alpha_2 e^{-\gamma\phi} (R_{GB}^2 + \mathcal{F}[\nabla\phi, R]) \right], \quad (2.4)$$

where we have introduced  $\phi = 2\gamma\hat{\phi}$  [18].  $R$  and  $R_{GB}^2$  are the Ricci scalar curvature and the Gauss-Bonnet curvature term with respect to the Einstein-frame metric  $g_{\mu\nu}$ , respectively. Because we have the Gauss-Bonnet term, if we start from the effective action in the string frame, there appears the additional complicated term  $\mathcal{F}$  in the Einstein frame, which is given by

$$\begin{aligned} \mathcal{F}[\nabla\phi, R] &= 4(D-3)\gamma R_{\mu\nu} \nabla^\mu \nabla^\nu \phi - 2(D-3)\gamma^2 R_{\mu\nu} (\nabla^\mu \phi)(\nabla^\nu \phi) - 2(D-3)\gamma R \nabla^2 \phi - \frac{1}{2}(D-3)_4 \gamma^2 R (\nabla\phi)^2 \\ &\quad - (D-2)_3 \gamma^2 (\nabla_\mu \nabla_\nu \phi)^2 + (D-2)_3 \gamma^2 (\nabla^2 \phi)^2 + (D-2)_3 \gamma^3 (\nabla^\mu \phi)(\nabla^\nu \phi)(\nabla_\mu \nabla_\nu \phi) \\ &\quad + \frac{1}{2}(D-2)(D-3)^2 \gamma^3 (\nabla^2 \phi)(\nabla\phi)^2 + \frac{1}{16}(D-1)_4 \gamma^4 [(\nabla\phi)^2]^2 \\ &= D(D-3)\gamma^2 G_{\mu\nu} \nabla^\mu \phi \nabla^\nu \phi + \frac{1}{2}(D-1)_3 \gamma^3 (\nabla^2 \phi)(\nabla\phi)^2 + \frac{1}{16}(D-1)_4 \gamma^4 [(\nabla\phi)^2]^2 + (\text{surface term}), \end{aligned} \quad (2.5)$$

where  $G_{\mu\nu}$  is the Einstein tensor. Here we have used a concise notation

$$(D-m)_n := (D-m)(D-m-1)\cdots(D-n), \quad (2.6)$$

with  $m$  and  $n$  being some integers ( $n > m$ ).

This term  $\mathcal{F}$  has not been sometimes considered in many literatures when cosmology or black hole solutions are studied in the Einstein frame [11–16]. However, if we start with the effective action in the string frame (2.1), there exists the complicated term (2.5) because the action with  $\mathcal{F}$  in the Einstein frame (2.4) is classically equivalent to the original one. We note that this does not mean that the theory in the Einstein frame without  $\mathcal{F}$  is not correct, but there is an intrinsic ambiguity in the theory. So it is interesting and important to study if this makes any difference in the obtained results.

In order to see the effects of this extra term  $\mathcal{F}$ , we study a black hole solution in this paper. For this purpose, we solve two sets of equations; one is a set of equations including the  $\mathcal{F}$  term, and the other is that without the  $\mathcal{F}$  term. We shall call the former and the latter the dilatonic Einstein-Gauss-Bonnet (DEGB) theory and the truncated one (TDEGB), respectively.

The action for TDEGB theory is given by

$$\mathcal{S}_T = \frac{1}{2\kappa_D^2} \int d^D x \sqrt{-g} \left[ R - \frac{1}{2}(\nabla\phi)^2 + \alpha_2 e^{-\gamma\phi} R_{GB}^2 \right], \quad (2.7)$$

Although one can solve the basic equations of the DEGB theory in the Einstein frame (2.4), it is easier to solve them in the string frame (2.1) and to transform the solutions in the string frame into those in the Einstein frame by the conformal transformation (2.3). This is the strategy we take here.

## III. DILATONIC EINSTEIN-GAUSS-BONNET MODEL IN THE STRING FRAME

### A. Basic equations in the string frame

First we present the basic equations in the string frame. To find a black hole solution, we assume a spherically symmetric and static spacetime, whose metric form is given by

$$d\hat{s}_D^2 = -e^{2\hat{\nu}} dt^2 + e^{2\hat{\lambda}} d\hat{r}^2 + e^{2\hat{\mu}} d\Omega_{D-2}^2, \quad (3.1)$$

where  $\hat{\nu}$ ,  $\hat{\lambda}$ , and  $\hat{\mu}$  are functions of the radial coordinate  $\hat{r}$ .  $d\Omega_{D-2}^2$  is the metric of  $(D-2)$ -dimensional unit sphere. We

derive the explicit form of the action with this ansatz as

$$\mathcal{S}_S = \frac{1}{2\kappa_D^2} \int d^D x e^{\hat{W}-2\hat{\phi}} \left\{ e^{-2\hat{\lambda}} [2(D-2)\hat{Y} + (D-2)_3\hat{A} - 4\hat{\phi}'\hat{\nu}'] + 4e^{-2\hat{\lambda}}\hat{\phi}'^2 + \tilde{\alpha}_2 e^{-4\hat{\lambda}} [(D-4)_5\hat{A}^2 + 4(D-4)\hat{Y}\hat{A} - 8\hat{\phi}'\hat{\nu}'\hat{A}] \right\}, \quad (3.2)$$

where we have introduced three variables  $\hat{Y}$ ,  $\hat{A}$ , and  $\hat{W}$  by

$$\begin{aligned} \hat{Y} &= -\left(\hat{\mu}'' + \hat{\mu}'^2 - \hat{\mu}'\hat{\lambda}'\right), \\ \hat{A} &= e^{2(\hat{\lambda}-\hat{\mu})} - \hat{\mu}'^2, \\ \hat{W} &= \hat{\nu} + \hat{\lambda} + (D-2)\hat{\mu}, \end{aligned} \quad (3.3)$$

and dropped the surface term. A prime denotes a derivative with respect to  $\hat{r}$ . For brevity, we have introduced the rescaled coupling constant as  $\tilde{\alpha}_2 := (D-2)_3\alpha_2$ , and in what follows, we will normalize the variables by it. Taking variations of the action with respect to  $\hat{\phi}$ ,  $\hat{\nu}$ ,  $\hat{\lambda}$ , and  $\hat{\mu}$ , we find the basic equations. Since we are interested in a black hole solution, it may be convenient to introduce new metric functions  $f$  and  $\delta$

as

$$ds^2 = -\hat{f}(\hat{r})e^{-2\hat{\delta}(\hat{r})}dt^2 + \frac{1}{\hat{f}(\hat{r})}d\hat{r}^2 + \hat{r}^2 d\Omega_{D-2}^2, \quad (3.4)$$

Here we have fixed one metric component as  $e^{2\hat{\mu}} = \hat{r}^2$  by using the gauge freedom. Using the new variables and defining the following variables by

$$\hat{h} := \hat{r}(\hat{f}' - 2\hat{f}\hat{\delta}'), \quad (3.5)$$

$$\hat{X} := \frac{1}{4\hat{f}^2\hat{r}^2} \left[ \hat{h}(\hat{f}'\hat{r} - \hat{h}) - 2\hat{f}(\hat{h}'\hat{r} - \hat{h}) \right], \quad (3.6)$$

the basic equations are written as

$$\begin{aligned} \hat{f}\hat{r}^4 F_{S(\hat{\phi})} &:= -2\left\{ \hat{r}^2 [(D-2)_3(1-\hat{f}) - (D-2)(\hat{f}'\hat{r} + \hat{h}) + 2\hat{X}\hat{f}\hat{r}^2 + 2(\hat{f}'\hat{r} + \hat{h})\hat{\phi}'\hat{r} + 4(D-2)\hat{f}\hat{\phi}'\hat{r} + 4\hat{f}(\hat{\phi}'' - \hat{\phi}'^2)\hat{r}^2] \right. \\ &\quad \left. + \tilde{\alpha}_2 [(D-4)_5(1-\hat{f})^2 - 2(D-4)(1-\hat{f})(\hat{f}'\hat{r} + \hat{h}) + 4\hat{X}(1-\hat{f})\hat{f}\hat{r}^2 + 2\hat{h}\hat{f}'\hat{r}] \right\} = 0, \end{aligned} \quad (3.7)$$

$$\begin{aligned} \hat{f}\hat{r}^4 F_{S(\hat{\nu})} &:= \hat{r}^2 [(D-2)_3(1-\hat{f}) - (D-2)(\hat{f}' - 4\hat{f}\hat{\phi}')\hat{r} + 4\hat{f}(\hat{\phi}'' - \hat{\phi}'^2)\hat{r}^2 + 2\hat{\phi}'\hat{f}'\hat{r}^2] \\ &\quad + \tilde{\alpha}_2 [(D-4)_5(1-\hat{f})^2 - 2(D-4)(1-\hat{f})(\hat{f}' - 4\hat{f}\hat{\phi}')\hat{r} \\ &\quad + 8\hat{f}(1-\hat{f})(\hat{\phi}'' - 2\hat{\phi}'^2)\hat{r}^2 + 4(1-3\hat{f})\hat{\phi}'\hat{f}'\hat{r}^2] = 0, \end{aligned} \quad (3.8)$$

$$\begin{aligned} \hat{f}\hat{r}^4 F_{S(\hat{\lambda})} &:= \hat{r}^2 [(D-2)_3(1-\hat{f}) - (D-2)(\hat{h} - 4\hat{f}\hat{\phi}'\hat{r}) + 2(\hat{h} - 2\hat{f}\hat{\phi}'\hat{r})\hat{\phi}'\hat{r}] \\ &\quad + \tilde{\alpha}_2 [(D-4)_5(1-\hat{f})^2 - 2(D-4)(1-\hat{f})(\hat{h} - 4\hat{f}\hat{\phi}'\hat{r}) + 4(1-3\hat{f})\hat{h}\hat{\phi}'\hat{r}] = 0, \end{aligned} \quad (3.9)$$

$$\begin{aligned} \hat{f}\hat{r}^4 F_{S(\hat{\mu})} &:= \hat{r}^2 [(D-2)_4(1-\hat{f}) - (D-2)_3(\hat{f}'\hat{r} + \hat{h}) + 4(D-2)_3\hat{f}\hat{\phi}'\hat{r} + 2(D-2)\hat{X}\hat{f}\hat{r}^2 \\ &\quad + 4(D-2)\hat{f}(\hat{\phi}'' - \hat{\phi}'^2)\hat{r}^2 + 2(D-2)(\hat{f}'\hat{r} + \hat{h})\hat{\phi}'\hat{r}] \\ &\quad + \tilde{\alpha}_2 [(D-4)_6(1-\hat{f})^2 - 2(D-4)_5(1-\hat{f})(\hat{f}'\hat{r} + \hat{h}) + 8(D-4)_5(1-\hat{f})\hat{f}\hat{\phi}'\hat{r} \\ &\quad + 4(D-4)\hat{X}(1-\hat{f})\hat{f}\hat{r}^2 + 8(D-4)\hat{f}(1-\hat{f})(\hat{\phi}'' - 2\hat{\phi}'^2)\hat{r}^2 + 4(D-4)(1-3\hat{f})(\hat{f}'\hat{r} + \hat{h})\hat{\phi}'\hat{r} \\ &\quad + 2(D-4)\hat{h}\hat{f}'\hat{r} - 8\hat{f}\hat{h}(\hat{\phi}'' - 2\hat{\phi}'^2)\hat{r}^2 - 8\hat{h}\hat{f}'\hat{\phi}'\hat{r}^2 + 16\hat{X}\hat{\phi}'\hat{f}^2\hat{r}^3] = 0. \end{aligned} \quad (3.10)$$

Because of the Bianchi identity, there is one relation between the above four functionals;  $F_{S(\hat{\phi})}$ ,  $F_{S(\hat{\nu})}$ ,  $F_{S(\hat{\lambda})}$ , and  $F_{S(\hat{\mu})}$ , i.e.,

$$\begin{aligned} &\hat{f}^{-1/2} \left( \hat{f}^{1/2} F_{S(\hat{\lambda})} \right)' \\ &= \frac{1}{\hat{r}} F_{S(\hat{\mu})} + \left( \frac{\hat{f}'}{2\hat{f}} - \hat{\delta}' \right) F_{S(\hat{\nu})} + \hat{\phi}' F_{S(\hat{\phi})}. \end{aligned} \quad (3.11)$$

That is, the above four Eqs. (3.7) ~ (3.10) are not independent. Hence, if we solve three of them, the remaining one equation is automatically satisfied.

## B. Boundary conditions

In order to find a black hole solution, we need the boundary conditions both at the event horizon and at the infinity. Since we are interested in an asymptotically “flat” spacetime, we

assume

$$\begin{aligned}\hat{f} &\rightarrow 1 - \left[ \frac{2\kappa_D^2}{(D-2)A_{D-2}} \right] \frac{\hat{M}}{\hat{r}^{D-3}}, \\ \hat{\delta} &\rightarrow \mathcal{O}\left(\frac{1}{\hat{r}^{D-3}}\right), \\ \hat{\phi} &\rightarrow \mathcal{O}\left(\frac{1}{\hat{r}^{D-3}}\right),\end{aligned}\quad (3.12)$$

as  $\hat{r} \rightarrow \infty$ , where

$$A_N = 2\pi^{(N+1)/2}/\Gamma[(N+1)/2], \quad (3.13)$$

is the area of  $N$ -dimensional unit sphere, and  $\hat{M}$  is a gravitational mass in the string frame.

At the event horizon ( $\hat{r}_H$ ), the metric function  $\hat{f}$  vanishes, i.e.,  $\hat{f}(\hat{r}_H) = 0$ . The variables and their derivatives must be finite at  $\hat{r}_H$ . Taking the limit of  $\hat{r} \rightarrow \hat{r}_H$ , we have three independent constraints from the basic equations:

$$\hat{\rho}_H^2 \left[ (D-2)_3 - 2(D-2)\hat{\xi}_H + 2\hat{\zeta}_H + 4\hat{\xi}_H\hat{\eta}_H \right] + \left[ (D-4)_5 - 4(D-4)\hat{\xi}_H + 4\hat{\zeta}_H + 2\hat{\xi}_H^2 \right] = 0, \quad (3.14)$$

$$\hat{\rho}_H^2 \left[ (D-2)_3 - (D-2)\hat{\xi}_H + 2\hat{\xi}_H\hat{\eta}_H \right] + \left[ (D-4)_5 - 2(D-4)\hat{\xi}_H + 4\hat{\xi}_H\hat{\eta}_H \right] = 0, \quad (3.15)$$

$$\begin{aligned}\hat{\rho}_H^2 \left[ (D-2)_4 - 2(D-2)_3\hat{\xi}_H + 2(D-2)\hat{\zeta}_H + 4(D-2)\hat{\xi}_H\hat{\eta}_H \right] \\ + \left[ (D-4)_6 - 4(D-4)_5\hat{\xi}_H + 4(D-4)\hat{\zeta}_H + 8(D-4)\hat{\xi}_H\hat{\eta}_H + 2(D-4)\hat{\xi}_H^2 - 8\hat{\xi}_H^2\hat{\eta}_H \right] = 0,\end{aligned}\quad (3.16)$$

where we have denoted the variables at the horizon with the subscript  $H$ , i.e.,  $\hat{\phi}_H, \hat{\phi}'_H, \hat{f}'_H, \hat{\delta}_H, \hat{\delta}'_H, (\hat{X}\hat{f})_H$  and so on, and introduced the dimensionless variables as

$$\hat{\rho}_H := \hat{r}_H/\tilde{\alpha}_2^{1/2}, \quad \hat{\xi}_H := \hat{r}_H\hat{f}'_H, \quad \hat{\eta}_H := \hat{r}_H\hat{\phi}'_H, \quad \hat{\zeta}_H := \hat{r}_H^2(\hat{X}\hat{f})_H. \quad (3.17)$$

Eliminating  $\hat{\xi}_H$  and  $\hat{\zeta}_H$  in Eqs. (3.14) ~ (3.16) [we assume that  $\hat{\xi}_H \neq 0$  and  $\hat{\zeta}_H \neq 0$ ], we find the quadratic equation for  $\hat{\eta}_H$ :

$$\hat{a}\hat{\eta}_H^2 + \hat{b}\hat{\eta}_H + \hat{c} = 0, \quad (3.18)$$

where

$$\begin{aligned}\hat{a} &= 4(\hat{\rho}_H^2 + 2) \left[ (D-2)_3\hat{\rho}_H^6 + 2(D^3 - 5D^2 + 2D + 14)\hat{\rho}_H^4 + 2(D-4)(3D^2 - 14D + 7)\hat{\rho}_H^2 + 4(D-3)_5 \right], \\ \hat{b} &= -2 \left[ (D-3)(D-2)^2\hat{\rho}_H^8 + (D-2)(7D^2 - 43D + 72)\hat{\rho}_H^6 + 2(D-4)(D^3 - 37D + 72)\hat{\rho}_H^4 \right. \\ &\quad \left. + 2(D-4)(D-5)(3D^2 - 5D - 16)\hat{\rho}_H^2 + 4(D-1)(D-5)(D-4)^2 \right], \\ \hat{c} &= -(D-1)\hat{\rho}_H^2 \left[ -(D-2)^3\hat{\rho}_H^4 + 4(D-4)(D-2)\hat{\rho}_H^2 + 2(D-4)^2(D+1) \right].\end{aligned}\quad (3.19)$$

The discriminant of the quadratic Eq. (3.18) depends on  $D$  and  $\hat{\rho}_H$ . If the discriminant is negative ( $\hat{D}_D := \hat{b}^2 - 4\hat{a}\hat{c} < 0$ ), there is no real value of  $\hat{\phi}'_H$ , which means that no regular horizon exists. The condition for the discriminant to be non-negative gives some constraint on  $\hat{\rho}_H^2$  for given  $D$ . Since  $\tilde{\alpha}_2$  is a fundamental coupling constant, it gives some condition on the horizon radius  $\hat{r}_H$ .

For  $D = 4 \sim 10$ , assuming  $\tilde{\alpha}_2 > 0$ , we find allowed values for the regular event horizon, which are summarized in Table I. There is a minimum horizon radius  $\hat{r}_H = 2.95712 \tilde{\alpha}_2^{1/2}$  in four-dimensional spacetime, while in five-dimensional and six-dimensional spacetimes, there is a small gap in the parameter space of horizon radius ( $1.03572 \tilde{\alpha}_2^{1/2} < \hat{r}_H < 2.55757 \tilde{\alpha}_2^{1/2}$  for five dimensions, and  $1.46781 \tilde{\alpha}_2^{1/2} < \hat{r}_H < 2.25772 \tilde{\alpha}_2^{1/2}$  for six dimensions) where there is no regular horizon. For spacetime of

dimensions higher than six, there is a regular horizon for any horizon radius.

#### IV. TRANSFORMATION TO THE EINSTEIN FRAME

Here we give the relation between the variables in the string frame and those in the Einstein frame. The metrics in both frames are given by Eq. (3.4) and

$$ds_D^2 = -f e^{-2\delta} dt^2 + \frac{1}{f} dr^2 + r^2 d\Omega_{D-2}^2, \quad (4.1)$$

respectively. The conformal transformation (2.3) or

$$\hat{g}_{\mu\nu} = \exp[\gamma\phi] g_{\mu\nu}, \quad (4.2)$$

TABLE I: The allowed values for a regular horizon radius are shown ( $\hat{\rho}_H := \hat{r}_H/\tilde{\alpha}_2^{1/2}$ ). The equality gives a double root of  $\phi'_H$ . There is a minimum radius in four dimensions. In five dimensions and six dimensions, there are gaps in which there is no regular horizon. For dimensions higher than six, a regular horizon always exists for any horizon radius.

$D$	Condition for regular horizon
4	$\hat{\rho}_H \geq 2.95712$
5	$\hat{\rho}_H \geq 2.55757$ or $\hat{\rho}_H \leq 1.03572$
6	$\hat{\rho}_H \geq 2.25772$ or $\hat{\rho}_H \leq 1.46781$
$7 \leq D \leq 10$	any values

gives the relation between the metric components as follows:

$$\hat{r} = \exp\left[\frac{\gamma\phi}{2}\right] r, \quad (4.3)$$

$$\hat{f} = \left(1 + \frac{\gamma r}{2} \frac{d\phi}{dr}\right)^2 f, \quad (4.4)$$

$$\hat{\delta} = \delta - \frac{\gamma\phi}{2} + \ln\left(1 + \frac{\gamma r}{2} \frac{d\phi}{dr}\right), \quad (4.5)$$

or inversely,

$$r = \exp[-\gamma^2\hat{\phi}]\hat{r}, \quad (4.6)$$

$$f = \left(1 - \gamma^2\hat{r} \frac{d\hat{\phi}}{d\hat{r}}\right)^2 \hat{f}, \quad (4.7)$$

$$\delta = \hat{\delta} + \gamma^2\hat{\phi} + \ln\left(1 - \gamma^2\hat{r} \frac{d\hat{\phi}}{d\hat{r}}\right). \quad (4.8)$$

Since the radial coordinates  $r$  and  $\hat{r}$  are related by Eq. (4.3) or Eq. (4.6), the horizon radii must be rescaled:

$$\begin{aligned} r_H &= \exp[-\gamma^2\hat{\phi}_H]\hat{r}_H, \\ \hat{r}_H &= \exp\left[\frac{\gamma\phi_H}{2}\right] r_H. \end{aligned} \quad (4.9)$$

The gravitational masses and the scalar charges are also rescaled as

$$\begin{aligned} GM &= G\hat{M} - (D-3)\gamma^2\hat{Q}_\phi, \\ G\hat{M} &= GM + \frac{(D-3)\gamma}{2}Q_\phi, \end{aligned} \quad (4.10)$$

$$Q_\phi = 2\gamma\hat{Q}_\phi, \quad (4.11)$$

where the scalar charges  $\hat{Q}_\phi$  in the string frame and  $Q_\phi$  in the Einstein frame are defined by the asymptotic behaviours

$$\begin{aligned} \hat{\phi} &\rightarrow \left[\frac{8\pi}{(D-2)A_{D-2}}\right] \frac{\hat{Q}_\phi}{\hat{r}^{D-3}}, \\ \phi &\rightarrow \left[\frac{8\pi}{(D-2)A_{D-2}}\right] \frac{Q_\phi}{r^{D-3}}, \end{aligned} \quad (4.12)$$

as  $\hat{r} \rightarrow \infty$  ( $r \rightarrow \infty$ ), respectively.

The lapse function  $\delta$  in the Einstein frame must drop as  $1/r^{2(D-3)}$ . As a result, we find

$$\begin{aligned} \hat{\delta} &\rightarrow -\left[\frac{8\pi\gamma}{A_{D-2}}\right] \frac{\hat{Q}_\phi}{\hat{r}^{D-3}}, \\ \delta &\rightarrow \mathcal{O}\left(\frac{1}{r^{2(D-3)}}\right), \end{aligned} \quad (4.13)$$

near infinity.

## V. THERMODYNAMIC VARIABLES

Before showing our numerical result, let us introduce thermodynamical variables of a black hole.

The Hawking temperature is given from the periodicity of the Euclidean time on the horizon as

$$\begin{aligned} \hat{T}_H &= \frac{1}{4\pi} \hat{f}'_H e^{-\hat{\delta}_H}, \\ T_H &= \frac{1}{4\pi} f'_H e^{-\delta_H}. \end{aligned} \quad (5.1)$$

Although we can define the Hawking temperature both in the string frame and in the Einstein frame, we find that both temperatures are the same by using the relation

$$\hat{f}'_H = \left(1 + \frac{\gamma r_H}{2} \phi'_H\right) e^{-\frac{\gamma\phi_H}{2}} f'_H. \quad (5.2)$$

As for a black hole entropy, it does not obey the Bekenstein-Hawking formula, i.e., a quarter of the area of event horizon, because we have the Gauss-Bonnet terms. According to the Wald's formula for a black hole entropy, which is defined by use of the Noether charge associated with the diffeomorphism invariance of the system [19], we find

$$S = -2\pi \int_\Sigma \frac{\partial \mathcal{L}}{\partial R_{\mu\nu\rho\sigma}} \epsilon_{\mu\nu} \epsilon_{\rho\sigma}, \quad (5.3)$$

where  $\Sigma$  is  $(D-2)$ -dimensional surface of the event horizon,  $\mathcal{L}$  is the Lagrangian density,  $\epsilon_{\mu\nu}$  denotes the volume element binormal to  $\Sigma$ .

For the effective action in the string frame (2.1), it gives

$$S_S = \frac{e^{-2\hat{\phi}_H} \hat{A}_H}{4} \left(1 + \frac{2\tilde{\alpha}_2}{\hat{r}_H^2}\right), \quad (5.4)$$

where  $\hat{A}_H$  is the area of the event horizon. Using the variables in the Einstein frame, this entropy is rewritten as [16]

$$S_S = \frac{A_H}{4} \left(1 + \frac{2\tilde{\alpha}_2}{r_H^2} e^{-\gamma\phi_H}\right). \quad (5.5)$$

We may look at the corrections to the Bekenstein-Hawking entropy ( $S_{\text{BH}} := A_H/4$ ) which is

$$S_S - S_{\text{BH}} = \frac{2\tilde{\alpha}_2}{r_H^2} e^{-\gamma\phi_H} \times S_{\text{BH}} > 0. \quad (5.6)$$

$S_S$  is always larger than  $S_{\text{BH}}$ .



## VI. BLACK HOLES IN THE DEGB THEORY

Now we present our numerical results.

Giving a horizon radius  $r_H$ , we solve the basic equations. To solve the equations numerically, we first set  $\delta_H = 0$ ,  $\phi_H = 0$ , and find the asymptotically flat spacetime. We then rescale the lapse function and the dilaton field as  $\tilde{\delta}(r) = \delta(r) - \delta(\infty)$  and  $\tilde{\phi}(r) = \phi(r) - \phi(\infty)$ . This is always possible because  $\delta$  and  $\phi$  appear only in the forms of their derivatives such as  $\delta'$  and  $\phi'$ . As a result, we can set  $\tilde{\delta}(r), \tilde{\phi}(r) \rightarrow 0$  for  $r \rightarrow \infty$ . Then in our actual solutions,  $\delta_H$  and  $\phi_H$  do not vanish. In what follows, for brevity, we omit the tilde of the variables.

Depending on the dimension, we classify our solutions into three types: (a) four dimensions ( $D = 4$ ), (b) five dimensions ( $D = 5$ ), and (c) six or higher dimensions ( $D = 6 \sim 10$ ).

### 1. Mass-area relation

First we show the relation between the black hole mass  $M$  and the horizon area  $A_H$  in Fig. 1. When we give the nu-

merical result, we show  $\bar{M} := \kappa_D^2 M$  for the mass instead of the gravitational mass  $M$ , because its value can be scaled as  $\tilde{\alpha}_2^{(D-3)/2}$  when we change the coupling constant  $\alpha_2$ . In the unit of  $\kappa_D = 1$ , both masses are equivalent. Hence, in what follows, for simplicity, we do not distinguish two masses and use  $M$  for both masses.

In the four-dimensional case, as shown in Fig.1 (a), there is the minimum radius below which there is no black hole ( $\hat{r}_{H(\min)} = 2.95712\tilde{\alpha}_2^{1/2}$ ). The ranges of the horizon radius where the black holes exist are shown in Table II and are narrower than those from the regularity condition in Table I in general, though the minimum radius in the string frame coincides with the value in Table I for four dimensions. The minimum mass of the black hole shown in Fig.1(a) is given by  $M_{\min} = 69.3511\tilde{\alpha}_2^{1/2}$ . Near this minimum mass, we find that the  $M$ - $A_H$  curve turns around, i.e., there are two black hole solutions for a given mass ( $M_{\min} \leq M < 72.3945\tilde{\alpha}_2^{1/2}$ ). We suspect that the larger black hole is stable, while the smaller one is unstable (see the later discussion about the entropy).

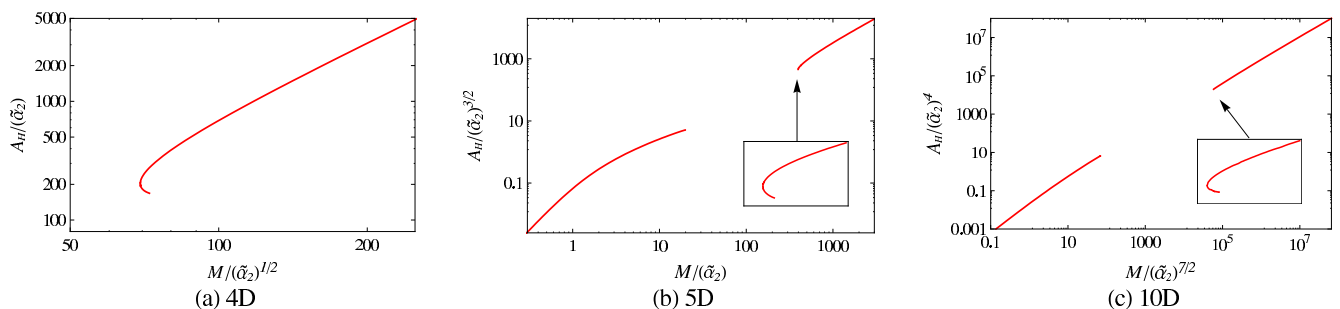


FIG. 1: The horizon area  $A_H$  in terms of the gravitational mass  $M$ . There appear mass gaps in five dimensions and ten dimensions. In four dimensions and in the L-branches of five dimensions and ten dimensions, we find the  $M$ - $A_H$  curves turn-around the minimum masses. We have two black hole solutions near the turn-around points. There is no turn-around behaviour in the S-branch.

TABLE II: The ranges of the horizon radii in which numerically solved black hole solutions exist both in the string frame ( $\hat{\rho}_H := \hat{r}_H / \tilde{\alpha}_2^{1/2}$ ) and in the Einstein frame ( $\rho_H := r_H / \tilde{\alpha}_2^{1/2}$ ). They are related by the conformal factor. There is a minimum radius in four dimensions. For dimensions higher than four dimensions, there is a gap, in which there is no regular black hole solution. The ranges of the horizon radius in the string frame should be compared with those in Table I

$D$	String frame	Einstein frame
4	$\hat{\rho}_H \geq 2.95712$	$\rho_H \geq 3.65726$
5	$\hat{\rho}_H \geq 2.55757$ or $\hat{\rho}_H \leq 0.647144$	$\rho_H \geq 2.84836$ or $\rho_H \leq 0.636670$
6	$\hat{\rho}_H \geq 2.26141$ or $\hat{\rho}_H \leq 0.780228$	$\rho_H \geq 2.44467$ or $\rho_H \leq 0.788059$
7	$\hat{\rho}_H \geq 2.13495$ or $\hat{\rho}_H \leq 0.835000$	$\rho_H \geq 2.25907$ or $\rho_H \leq 0.842271$
8	$\hat{\rho}_H \geq 2.12365$ or $\hat{\rho}_H \leq 0.848702$	$\rho_H \geq 2.21291$ or $\rho_H \leq 0.853517$
9	$\hat{\rho}_H \geq 2.15406$ or $\hat{\rho}_H \leq 0.842414$	$\rho_H \geq 2.22300$ or $\rho_H \leq 0.845275$
10	$\hat{\rho}_H \geq 2.20216$ or $\hat{\rho}_H \leq 0.827220$	$\rho_H \geq 2.25818$ or $\rho_H \leq 0.828790$

In the five-dimensional case, there appears new type of solutions near the zero-mass region as shown in Fig. 1(b). We find two mass ranges: one has the smaller masses (S-branch), and the other has the larger masses (L-branch). There is a

mass gap between these two branches. It has been expected from the results which we found from the regularity condition for the horizon (see Table I). The L-branch is similar to the solutions in the four-dimensional case. There exists the lower

mass bound. Near the minimum mass ( $M_{\min}^{(L)} = 395.862\tilde{\alpha}_2$ ), we find two black hole solutions in the range of  $M_{\min}^{(L)} < M < 395.880\tilde{\alpha}_2$  (see the enlarged figure in Fig. 1(b)). The minimum radius in this branch is found by the existence condition of the regular horizon, i.e.,  $\hat{r}_{H(\min)} = 2.55757\tilde{\alpha}_2^{1/2}$  (Compare Tables I and II) just as in the four-dimensional case. In the S-branch, we find the maximum mass ( $M_{\max}^{(S)} = 19.7733\tilde{\alpha}_2$ ). There is no turn-around behaviour near the maximum mass in the S-branch. As the horizon radius approaches zero, the gravitational mass vanishes. We find  $M \approx 0.100295\tilde{\alpha}_2^{1/2}r_H$  in the zero-mass limit. (Note that  $M \propto r_H^2$  in the case of five-dimensional Schwarzschild black hole.)

In dimensions higher than five, we find the similar structures; i.e., there are two branches (the S- and L-branches). However, in the L-branch, the minimum radius is not given by the regularity condition (see Tables I and II). In fact, for  $D \geq 7$ , we find a gap in the range of black hole radii in numerical solutions, but the regular horizon condition is always satisfied for any horizon radii. In this gap, we cannot find any asymptotically flat black hole solution, although the horizon can be regular. The L-branch shows the similar properties to those in the four-dimensional or five-dimensional case. In the S-branch in ten dimensions, we find  $M_{\max}^{(S)} = 68.6614\tilde{\alpha}_2^{7/2}$ , and  $M \approx 84.1890\tilde{\alpha}_2 r_H^5$  in the zero-mass limit. (Note that  $M \propto r_H^7$  in the case of ten-dimensional Schwarzschild black hole.)

We cannot make definite statement about what happens in the region of a mass gap. Since there is no static black hole, the spacetime may be always dynamical losing the mass energy and eventually reaching the S-branch, or it may evolve into a naked singularity.

## 2. Thermodynamics

Next we present the thermodynamical variables. First we give the entropy in terms of the gravitational mass  $M$  in Fig. 2. The entropy behaves very similar to the area of the horizon, although there is a correction to the Bekenstein-Hawking entropy, which is also shown by the (blue) dotted line as a ref-

erence in the figure. In particular, we find turn-around behaviours near the minimum masses in four dimensions and in the L-branches of five dimensions and ten dimensions. Near the minimum points, we have two black holes for a given mass. The larger black hole has the larger entropy, and then we expect that it is dynamically stable. On the other hand, the smaller black hole has the smaller entropy, and then we expect that it is dynamically unstable.

We also show the temperatures of the black holes in Fig. 3. The temperature in four dimensions is always finite and shows the turn-around behaviour near the minimum mass. At this turning point, we expect a change of stability (see the discussion in [20]). When the black hole evaporates via the Hawking radiation, the mass decreases. Although the temperature is finite, it does not vanish at the minimum mass, and the evaporation never stops at the minimum mass. We may find a naked singularity.

In five dimensions and higher dimensions, we find the same behaviour as for the L-branch. In the S-branch, however, the temperature in five dimensions is always finite and vanishes at the zero-mass limit. Then the black hole may disappear via the Hawking radiation.

On the other hand, the behaviour is very different in dimensions higher than five. The temperature in ten dimensions diverges as  $M \rightarrow 0$ . We find the same behaviour for the case of  $D = 6 \sim 9$ . The evaporation never stops even near the zero-mass limit. Rather the black hole may explode via the Hawking radiation.

As a result, we can classify our solutions into three types: (a)  $D = 4$ , (b)  $D = 5$ , and (c)  $D = 6 \sim 10$ .

The reason why we have three types may be understood as follows: The Gauss-Bonnet curvature in four dimensions becomes a total divergence if there is no dilaton field, and then it does not give any contribution in the basic equations. Even if we include a dilaton field, we expect the dynamical properties of the Gauss-Bonnet term in four dimensions is very much different from those in the case of  $D \geq 5$ , in which the Gauss-Bonnet term gives a significant change in the basic equations without a dilaton field.

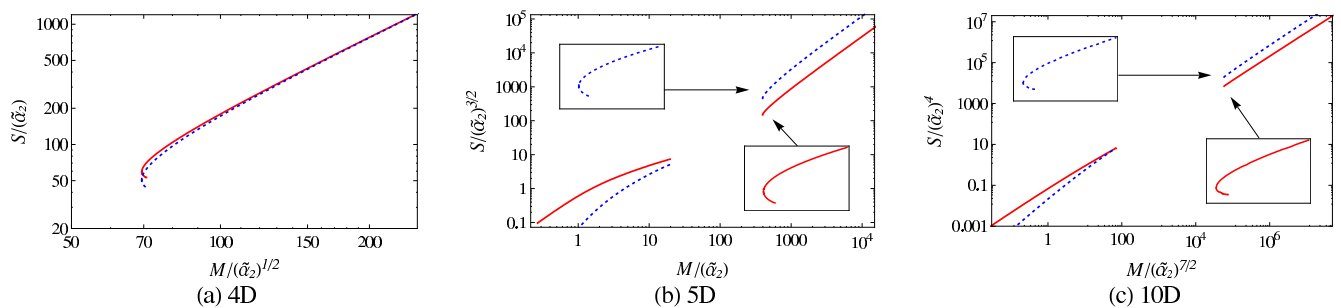


FIG. 2: The entropies  $S_S$  of black holes in DEGB in terms of the mass  $M$  by the solid (red) line for (a)  $D = 4$ , (b)  $D = 5$ , and (c)  $D = 10$ . As a reference, we also show the Bekenstein-Hawking entropy  $S_{\text{BH}} = A_H/4$  by the (blue) dotted line.

Five dimensions and six dimensions are also different from other higher dimensions, because the Gauss-Bonnet term is the highest Lovelock term in five dimensions and six dimensions, while in higher dimensions ( $D = 7 \sim 10$ ), there exist higher Lovelock terms. There may also be a big difference between odd and even dimensions. Hence, we expect four types: four dimensions, five dimensions and six dimensions, and higher dimensions ( $D = 7 \sim 10$ ). However, it turns out that the solutions

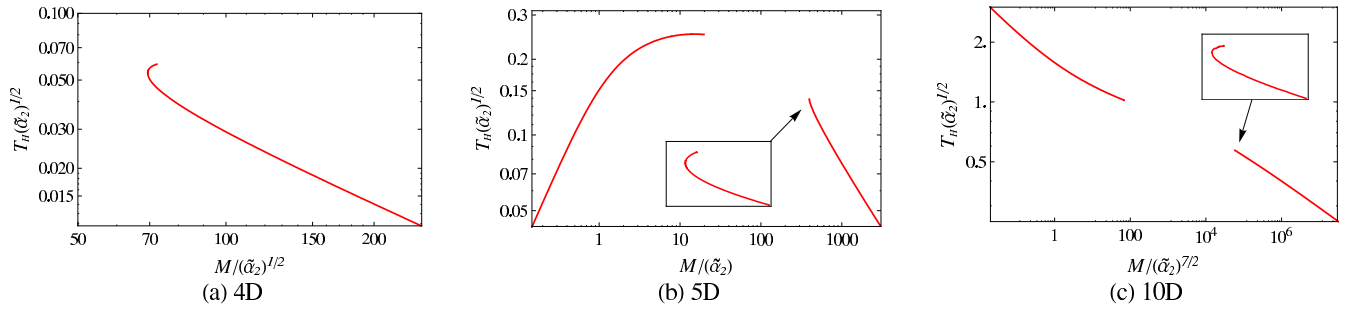


FIG. 3: Temperatures of black holes in DEGB for (a)  $D = 4$ , (b)  $D = 5$ , and (c)  $D = 10$ .

in six dimensions and higher dimensions look similar. As a result, we find three types.

### 3. Configuration of the metric and dilaton field

Here, we show the behaviour of the mass function defined by  $m(r) = r^{D-3}(1 - f(r))/2$ , which approaches the ADM(Arnott-Deser-Miser) mass at infinity, the lapse function  $\delta(r)$  and the dilaton field  $\phi(r)$ , for several values of the horizon radii in Fig. 4 in four dimensions.

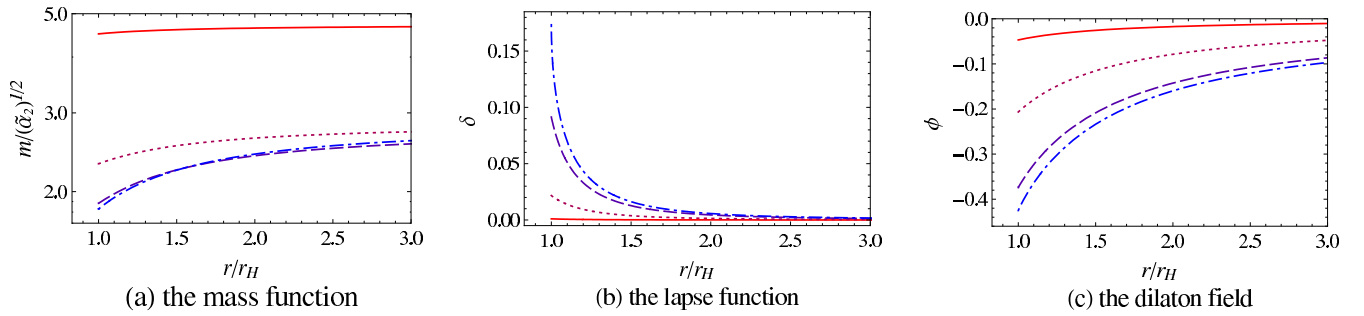


FIG. 4: The solution of the four-dimensional black hole. We choose the following four values for the horizon radius:  $r_H = 8.80392\tilde{\alpha}_2^{1/2}$  (solid),  $4.16383\tilde{\alpha}_2^{1/2}$  (dotted),  $3.12416\tilde{\alpha}_2^{1/2}$  (dashed), and  $2.95712\tilde{\alpha}_2^{1/2}$  (dot-dashed).

In four dimensions, we find that the mass function, lapse function and dilaton field behave monotonously smooth ( see Fig. 4). For the solution with minimum horizon radius, however, the second derivative of the dilaton field diverges (Fig. 4 (c)). We show the Kretschmann curvature invariant defined by  $K := R_{\mu\nu\rho\sigma}R^{\mu\nu\rho\sigma}$  for several radii in Fig. 5 (a). We can see the curvature at the horizon increases rapidly near the minimum radius. We find the curvature singularity on the horizon in the limit of  $M \rightarrow M_{\min}$ .

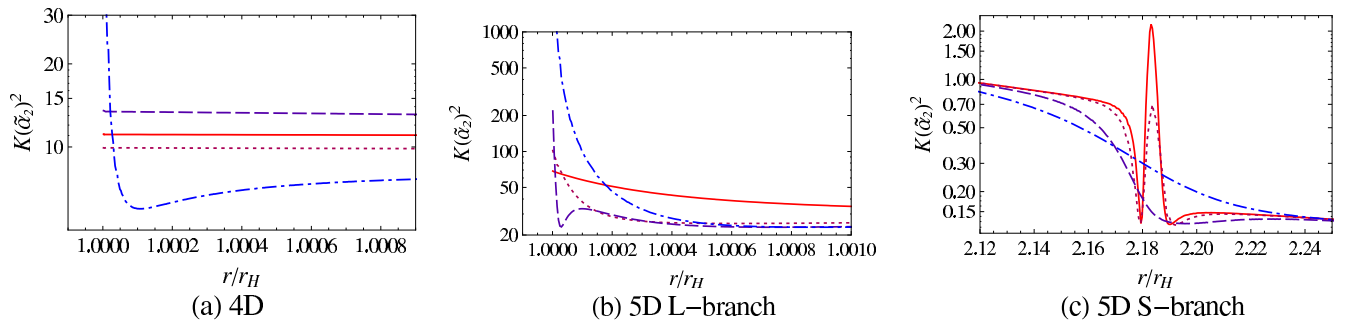


FIG. 5: The Kretschmann curvature invariants for several horizon radii in four dimensions and five dimensions. We choose four values of the horizon radius in four dimensions:  $r_H = 3.66391\tilde{\alpha}_2^{1/2}$  (solid),  $3.65865\tilde{\alpha}_2^{1/2}$  (dotted),  $3.65751\tilde{\alpha}_2^{1/2}$  (dashed), and  $3.65726\tilde{\alpha}_2^{1/2}$  (dot-dashed), in the L-branch of five dimensions:  $r_H = 2.84950\tilde{\alpha}_2^{1/2}$  (solid),  $2.84861\tilde{\alpha}_2^{1/2}$  (dotted),  $2.84841\tilde{\alpha}_2^{1/2}$  (dashed), and  $2.84837\tilde{\alpha}_2^{1/2}$  (dot-dashed), and in the S-branch of five dimensions:  $r_H = 0.636663\tilde{\alpha}_2^{1/2}$  (solid),  $0.636652\tilde{\alpha}_2^{1/2}$  (dotted),  $0.636591\tilde{\alpha}_2^{1/2}$  (dashed),  $0.636400\tilde{\alpha}_2^{1/2}$  (dot-dashed). In four dimensions and the L-branch of five dimensions, the curvature invariant increases rapidly near the horizon, and below the minimum radius, we will find a curvature singularity. On the other hand, in the S-branch of five dimensions, we find a strange behaviour of the curvature invariant near  $r \approx 2.18r_H$ , but it does not diverge near the horizon.



For the L-branch of the five-dimensional black holes, we find very similar behaviours to the case of four dimensions. For the solution with minimum horizon radius, the second derivative of the dilaton field diverges. The Kretschmann curvature invariant also diverges at the horizon in the limit of  $M \rightarrow M_{\min}^{(L)}$ , as shown in Fig. 5 (b).

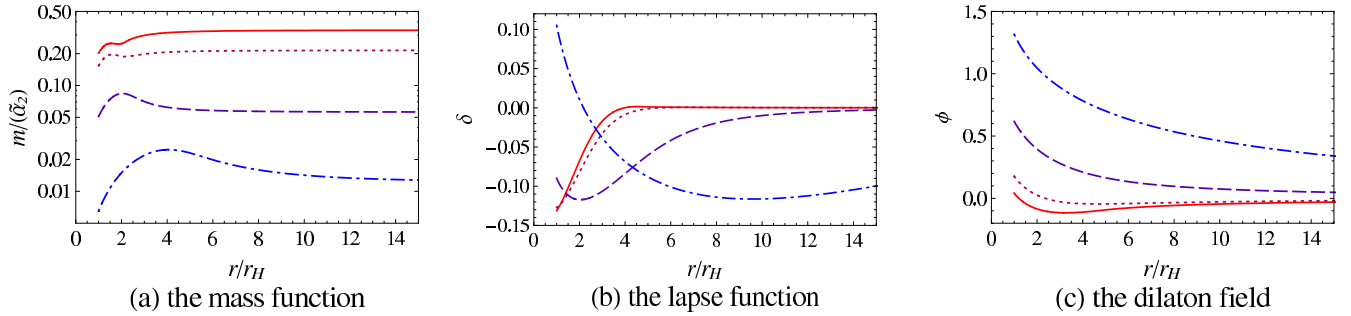


FIG. 6: The solution of the S-branch of the five-dimensional black hole. We choose the following four values for the horizon radius:  $r_H = 0.636670\tilde{\alpha}_2^{1/2}$  (solid),  $0.554630\tilde{\alpha}_2^{1/2}$  (dotted),  $0.319473\tilde{\alpha}_2^{1/2}$  (dashed),  $0.114232\tilde{\alpha}_2^{1/2}$  (dot-dashed). Near the maximum mass of the S-branch, we find some irregular behaviour just outside of the horizon.

In the S-branch, however, we find somewhat different result. As we see in Fig. 6, we find some irregular behaviour just outside of the horizon ( $r \sim 2r_H$ ) for the black holes with  $r_H = 0.636670\tilde{\alpha}_2^{1/2}$  (the solid line) and  $0.554630\tilde{\alpha}_2^{1/2}$  (the dotted line), and the corresponding masses ( $M = 19.7733\tilde{\alpha}_2$  and  $12.7352\tilde{\alpha}_2$ ) are close to the maximum values  $M_{\max}^{(S)} (= 19.7733\tilde{\alpha}_2)$  in the S-branch. We show the Kretschmann curvature invariant for several radii in Fig. 5 (c). Although we find a strange behaviour of the curvature invariant around  $r \approx 2.18r_H$ , the curvature does not seem to diverge on the horizon. We suspect that the point with the irregular behaviour outside the horizon will become a singularity in the limit of  $M \rightarrow M_{\max}^{(S)}$ .

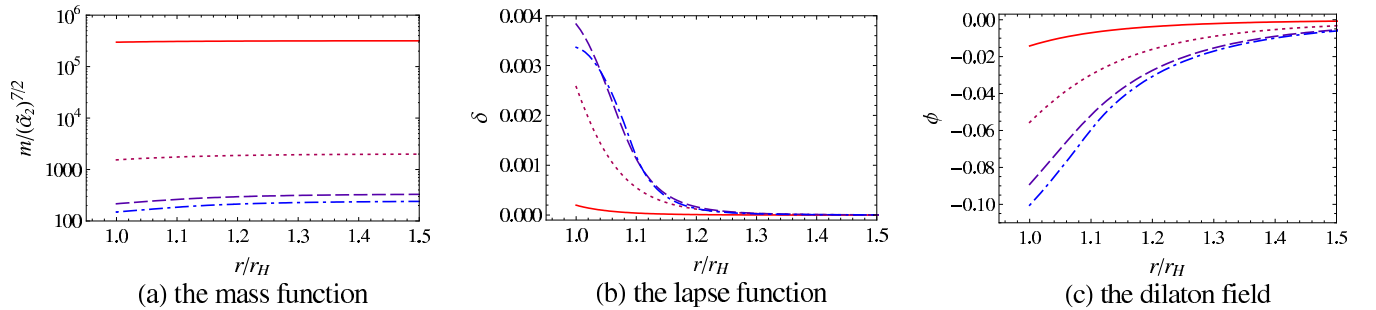


FIG. 7: The solution of the L-branch of the ten-dimensional black hole. We choose the following four values for the horizon radius:  $r_H = 6.683666\tilde{\alpha}_2^{1/2}$  (solid),  $3.150271\tilde{\alpha}_2^{1/2}$  (dotted),  $2.379547\tilde{\alpha}_2^{1/2}$  (dashed), and  $2.258180\tilde{\alpha}_2^{1/2}$  (dot-dashed). Near the minimum mass of the L-branch, the lapse function and the dilaton field diverge at the horizon. The singularity appears on the horizon in the limit of  $M \rightarrow M_{\min}^{(L)}$ .

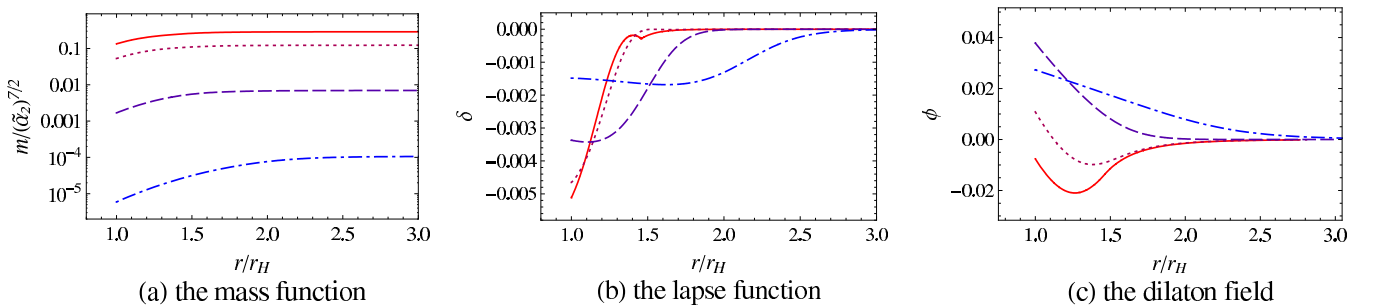


FIG. 8: The solution of the S-branch of the ten-dimensional black hole. We choose the following four values for the horizon radius:  $r_H = 0.4135451\tilde{\alpha}_2^{1/2}$  (solid),  $0.1639727\tilde{\alpha}_2^{1/2}$  (dotted),  $0.0645152\tilde{\alpha}_2^{1/2}$  (dashed), and  $0.03157994\tilde{\alpha}_2^{1/2}$  (dot-dashed).

Next we depict the mass function, lapse function and dilaton field in ten dimensions in Figs. 7 and 8. We find the very different behaviour in the L-branch from the four-dimensional

case or from the L-branch in five dimensions. In the L-branch, the lapse function and the dilaton field does not diverge near the horizon in the limit of  $r_H \rightarrow r_{\min}^{(L)}$ . We show the

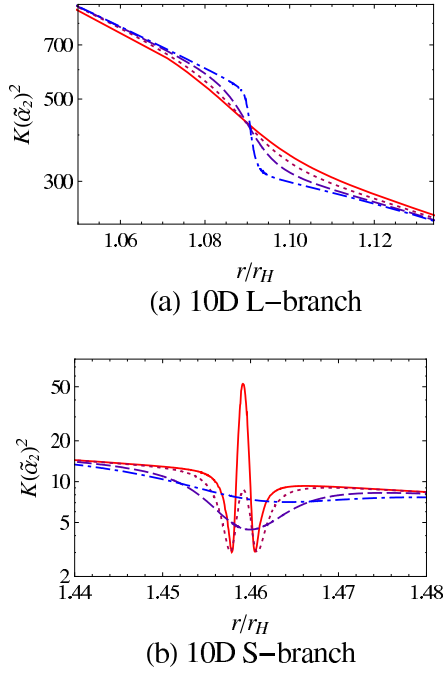


FIG. 9: The curvature invariants for several masses in ten dimensions. We choose the following four values for the horizon radius in the L-branch:  $r_H = 2.27983\tilde{\alpha}_2^{1/2}$  (solid),  $2.26830\tilde{\alpha}_2^{1/2}$  (dotted),  $2.26116\tilde{\alpha}_2^{1/2}$  (dashed), and  $2.25820\tilde{\alpha}_2^{1/2}$  (dot-dashed). In the S-branch:  $r_H = 0.828778\tilde{\alpha}_2^{1/2}$  (solid),  $0.828748\tilde{\alpha}_2^{1/2}$  (dotted),  $0.828366\tilde{\alpha}_2^{1/2}$  (dashed), and  $0.826771\tilde{\alpha}_2^{1/2}$  (dot-dashed). Near the minimum radius in the L-branch, the invariant does not diverge, but evolves into a “gravitational shock wave” at  $r \approx 1.09r_H$  in the limit of minimum radius. In the S-branch, a strange behaviour appears near  $r \approx 1.46r_H$  outside the horizon. It may evolve into a singularity in the limit of  $M \rightarrow M_{\max}^{(S)}$ .

Kretschmann curvature invariant in Fig. 9 (a). There appears a discontinuity in the curvature invariant around  $r \approx 1.09r_H$  for  $r_H = 2.25818\tilde{\alpha}_2^{1/2}$ . This point does not evolve into the divergence of the curvature even in the limit of  $r_H \rightarrow r_{\min}^{(L)}$ . We may regard it as a “gravitational shock wave”, where we have a curvature discontinuity. It is a new type of singularity. The reason why we find the minimum radius in the L-branch is

different from the minimum radius found by the regular horizon condition is that the “gravitational shock wave” appears first outside of the horizon before the singularity appears on the horizon when we take the limit of  $r_H \rightarrow r_{\min}^{(L)}$ .

In the S-branch, we also find the similar behaviour to the S-branch in five dimensions. Some irregular behaviour appears around  $r \approx 1.46r_H$  outside of the horizon near the maximum mass  $M_{\max}^{(S)}$ . It may evolve into a singularity in the limit of  $M \rightarrow M_{\max}^{(S)}$ .

Now we can summarize our results as follows: For the four dimensions and the L-branch in five dimensions, there is a minimum radius, below which the curvature diverges on the horizon. When  $D \geq 6$ , the singularity of the gravitational shock-wave appears in the L-branch below the minimum radius. On the other hand, for the S-branch of five and higher dimensions, there exists a maximum mass, beyond which a black hole does not exist, and a singularity may appear outside the horizon.

## VII. TRUNCATED DILATONIC EINSTEIN-GAUSS-BONNET MODEL

In this section, we discuss the truncated Einstein-Gauss-Bonnet model, whose action is given by Eq. (2.7). The properties of black hole solutions in the TDEGB model with  $\gamma = \frac{1}{2}$  are studied in [16]. This value of the coupling constant is obtained in ten dimensions. If we start from the effective action in the string frame in  $D$  dimensions, we have the different value, which is  $\gamma = \sqrt{2/(D-2)}$ , in the Einstein frame. Here we choose this value of the coupling constant for the TDEGB model. The difference of two models originates from the compactification. We find some qualitative differences in thermodynamical properties in the TDEGB models with these two coupling constants (see the discussion in Sec. IX). In what follows in the text, we show the black hole solutions and their properties in the TDEGB model with  $\gamma = \sqrt{2/(D-2)}$ .

### A. Basic equations

The field equations are given by

$$fr^2 F_{T(\phi)} := \frac{1}{2}(f'r + h + 2(D-2)f)\phi'r + f\phi''r^2 - \gamma B[(D-4)_5(1-f)^2 - 2(D-4)(1-f)(f'r + h) + 4Xf(1-f)r^2 + 2hf'r] = 0, \quad (7.1)$$

$$fr^2 F_{T(\nu)} := (D-2)_3(1-f) - (D-2)f'r - \frac{1}{2}f\phi'^2r^2 + B[(D-4)_5(1-f)^2 - 2(D-4)(1-f)(f' - 2\gamma f\phi')r + 4\gamma f(1-f)(\phi'' - \gamma\phi'^2)r^2 + 2\gamma(1-3f)\phi'f'r^2] = 0, \quad (7.2)$$

$$fr^2 F_{T(\lambda)} := (D-2)_3(1-f) - (D-2)h + \frac{1}{2}f\phi'^2r^2 + B[(D-4)_5(1-f)^2 - 2(D-4)(1-f)(h - 2\gamma f\phi')r + 2\gamma h(1-3f)\phi'r] = 0, \quad (7.3)$$

$$fr^2 F_{T(\mu)} := (D-2)_4(1-f) - (D-2)_3(f'r + h) + 2(D-2)Xfr^2 - \frac{1}{2}(D-2)f\phi'^2r^2 + B[(D-4)_6(1-f)^2 - 2(D-4)_5(1-f)(f'r + h) + 4\gamma(D-4)_5f(1-f)\phi'r + 4(D-4)(1-f)Xfr^2 + 4\gamma(D-4)f(1-f)(\phi'' - \gamma\phi'^2)r^2 + 2(D-4)hf'r + 2\gamma(D-4)(1-3f)(f'r + h)\phi'r - 4\gamma fh(\phi'' - \gamma\phi'^2)r^2 - 4\gamma h\phi'f'r^2 + 8\gamma\phi'Xf^2r^3] = 0. \quad (7.4)$$

where

$$X(r) := \frac{1}{4f^2r^2} [h(f'r - h) - 2f(h'r - h)], \quad (7.5)$$

$$B(r) := r^{-2}\tilde{\alpha}_2 e^{-\gamma\phi}, \quad (7.6)$$

$$h(r) := r(f' - 2f\delta'). \quad (7.7)$$

The Bianchi identity gives one relation between these four functionals:

$$\begin{aligned} & f^{-1/2} \left( f^{1/2} F_{T(\lambda)} \right)' \\ &= \frac{1}{r} F_{T(\mu)} + \left( \frac{f'}{2f} - \delta' \right) F_{T(\nu)} + \phi' F_{T(\phi)}. \end{aligned} \quad (7.8)$$

Hence if one solve three of them, the remaining one equation is automatically satisfied.

### B. Boundary conditions

As we discussed in Sec. III B, we need the boundary conditions both at the event horizon ( $r = r_H$ ) and at the infinity ( $r = \infty$ ). The asymptotical ‘‘flatness’’ implies

$$\begin{aligned} f &\rightarrow 1 - \left[ \frac{2\kappa_D^2}{(D-2)A_{D-2}} \right] \frac{M}{r^{D-3}}, \\ \delta &\rightarrow \mathcal{O} \left( \frac{1}{r^{2(D-3)}} \right), \\ \phi &\rightarrow \mathcal{O} \left( \frac{1}{r^{D-3}} \right), \end{aligned} \quad (7.9)$$

The regularity conditions of the event horizon are now

$$\bar{\rho}_H^2 \xi_H \eta_H - \gamma [(D-4)_5 - 4(D-4)\xi_H + 4\zeta_H + 2\xi_H^2] = 0, \quad (7.10)$$

$$\bar{\rho}_H^2 [(D-2)_3 - (D-2)\xi_H] + [(D-4)_5 - 2(D-4)\xi_H + 2\gamma\xi_H\eta_H] = 0, \quad (7.11)$$

$$\begin{aligned} & \bar{\rho}_H^2 [(D-2)_4 - 2(D-2)_3\xi_H + 2(D-2)\zeta_H] \\ & + [(D-4)_6 - 4(D-4)_5\xi_H + 4(D-4)\zeta_H + 4\gamma(D-4)\xi_H\eta_H + 2(D-4)\xi_H^2 - 4\gamma\xi_H^2\eta_H] = 0, \end{aligned} \quad (7.12)$$

where

$$\bar{\rho}_H := r_H e^{\gamma\phi_H/2} / \tilde{\alpha}_2^{1/2}, \quad \xi_H := r_H f'_H, \quad \eta_H := r_H \phi'_H, \quad \text{and} \quad \zeta_H := r_H^2 (Xf)_H. \quad (7.13)$$

Eliminating  $\xi_H$  and  $\zeta_H$  in Eqs. (7.10) ~ (7.12) [we assume that  $\xi_H \neq 0$  and  $\zeta_H \neq 0$ ], we find the quadratic equation for  $\eta_H$ :

$$a\eta_H^2 + b\eta_H + c = 0, \quad (7.14)$$

where

$$\begin{aligned} a &= 2\gamma \left[ ((D-2)_3 \bar{\rho}_H^2 + (D-4)_5) ((D-2) \bar{\rho}_H^2 + 2(D-4)) + 2\gamma^2 ((D-2)(D-4)(3D-11) \bar{\rho}_H^2 + 4(D-3)_5) \right], \\ b &= - \left[ ((D-2)_3 \bar{\rho}_H^2 + (D-4)_5) ((D-2) \bar{\rho}_H^2 + 2(D-4))^2 \right. \\ &\quad \left. - 4\gamma^2 (D-1)(D-4) ((D-2)^2 \bar{\rho}_H^4 + 2(D-2) \bar{\rho}_H^2 - 2(D-4)_5) \right], \\ c &= \gamma (D-1) 2 \bar{\rho}_H^2 [(D-2)^3 \bar{\rho}_H^4 - 4(D-2)(D-4) \bar{\rho}_H^2 - 2(D+1)(D-4)^2], \end{aligned} \quad (7.15)$$

as  $r \rightarrow \infty$ .  $M$  is a gravitational mass in the Einstein frame. Since the weak equivalence principle is satisfied in the Einstein frame, the lapse must drop faster than the gravitational potential ( $f - 1$ ).

TABLE III: The allowed values for the regular horizon radius are shown. The equality gives a double root of  $\phi'_H$ . There is a minimum radius in four dimensions. In five dimensions and six dimensions, there are gaps in which there is no regular horizon. For dimensions higher than six, there is a regular horizon for any horizon radius.  $\bar{\rho}_H := r_H e^{\gamma\phi_H/2} / \tilde{\alpha}_2^{1/2}$ .

$D$	Condition for regular horizon
4	$\bar{\rho}_H \geq 1.86121$
5	$\bar{\rho}_H \geq 1.45828$ or $\bar{\rho}_H \leq 0.962882$
$6 \leq D \leq 10$	any values

At the event horizon ( $r_H$ ), the metric function  $f$  vanishes, i.e.  $f(r_H) = 0$ . The variables and their derivatives must be finite at  $r_H$ .

For  $D = 4 \sim 10$ , assuming  $\tilde{\alpha}_2 > 0$  and imposing the dis-

criminant is non-negative ( $\mathcal{D}_D := b^2 - 4ac \geq 0$ ), we find

the allowed values for the regular event horizon, which are summarized in Table III. There is a minimum horizon radius  $r_H = 1.86121 \tilde{\alpha}_2^{1/2} e^{-\gamma\phi_H/2}$  in four-dimensional spacetime, while in five-dimensional spacetime, there is a small gap in the parameter space of horizon radius ( $0.962882 \tilde{\alpha}_2^{1/2} e^{-\gamma\phi_H/2} < r_H < 1.45828 \tilde{\alpha}_2^{1/2} e^{-\gamma\phi_H/2}$ ) where there is no regular horizon. For higher dimensional spacetime than five dimensions, there is a regular horizon for any horizon radius.

### VIII. COMPARISON WITH TDEGB AND EGB

Now we compare the properties of the black hole solutions in the DEGB and TDEGB models. We also show the results in the EGB model as a reference.

#### A. Mass-area relation

First we show the mass-area relations of black holes in Fig. 10. The solid (red) line, dashed (green) line, and dot-dashed (black) line correspond to the DEGB, TDEGB, and EGB models, respectively.

In four dimensions, there exists the minimum finite radius,  $r_{H(\min)} = 3.65726\tilde{\alpha}_2^{1/2}$  and  $3.138439\tilde{\alpha}_2^{1/2}$ , and minimum mass,  $M_{\min}^{(\text{DEGB})} = 69.3511\tilde{\alpha}_2^{1/2}$  and  $M_{\min}^{(\text{TDEGB})} = 42.7128\tilde{\alpha}_2^{1/2}$ , both for the DEGB and TDEGB models, respectively. There is no qualitative difference. A turning point appears at the minimum mass, near where two black holes exist in a small mass range ( $M_{\min}^{(\text{DEGB})} \leq M < 72.3945\tilde{\alpha}_2^{1/2}$  for DEGB and  $M_{\min}^{(\text{TDEGB})} \leq M < 42.7152\tilde{\alpha}_2^{1/2}$  for TDEGB). In the EGB model, it is just a Schwarzschild black hole because the Gauss-Bonnet term is a total divergence. It is completely different from the other two.

In five dimensions, the result changes drastically (see

Fig. 10(b)). For the EGB model, the mass-area relation is very simple (the dot-dashed line). The area increases monotonically with respect to the mass, and there exists a minimum finite mass ( $M_{\min}^{(\text{EGB})} = 2\pi^2\tilde{\alpha}_2$ ). In the TDEGB model, the mass-area relation is also monotonic, but it splits up into two branches (the S- and L-branches) shown by the dashed (green) line just as in the DEGB model (the solid [red] line). The ranges are  $M_{\min}^{(\text{S})} < M < M_{\max}^{(\text{S})}$  and  $M > M_{\min}^{(\text{L})}$  for the S- and L-branches, respectively, where  $M_{\min}^{(\text{S})} := 10.8051\tilde{\alpha}_2$ ,  $M_{\max}^{(\text{S})} := 27.4615\tilde{\alpha}_2$ , and  $M_{\min}^{(\text{L})} := 142.382\tilde{\alpha}_2$ . So there exists a finite minimum mass ( $M_{\min}^{(\text{S})}$ ), and the area in the L-branch increase monotonically without any turning point as well as that in the S-branch. However, in the case of the DEGB model, as we discussed in Sec. VI, the black holes exist from zero mass, and there appears a mass gap ( $M_{\max}^{(\text{S})} = 19.7733\tilde{\alpha}_2 < M < M_{\min}^{(\text{L})} = 395.862\tilde{\alpha}_2$ ) where no black hole exists. In the L-branch of the DEGB model, we find two black hole solutions with the different horizon radii but with the same mass in the range of  $M_{\min}^{(\text{L})} < M < 395.880\tilde{\alpha}_2$ . The smaller-radius black hole may be unstable because the entropy is also smaller.

In ten dimensions, the mass-area relations are almost the same for the DEGB, TDEGB, and EGB models. However there is a qualitative difference between the DEGB model and the TDEGB (or EGB) model. In the TDEGB (or EGB) model, the area increases monotonically with respect to the mass from zero to infinity. The mass vanishes at zero area. However, in the DEGB model, there exists a gap in the range of mass ( $M_{\max}^{(\text{S})} = 68.6614\tilde{\alpha}_2^{7/2} \leq M < M_{\min}^{(\text{L})} = 58647.5\tilde{\alpha}_2^{7/2}$ ), and a turning point appears near the minimum mass  $M_{\min}^{(\text{L})}$ . There exist two different solution with the same mass, in the range of mass ( $M_{\min}^{(\text{L})} < M < M_{\min}^{(\text{L})} + 1.56019 \times 10^{-5}\tilde{\alpha}_2^{7/2}$ ). The behaviour is the same as that in five dimensions.

We also find the same behaviours in six to nine dimensions.

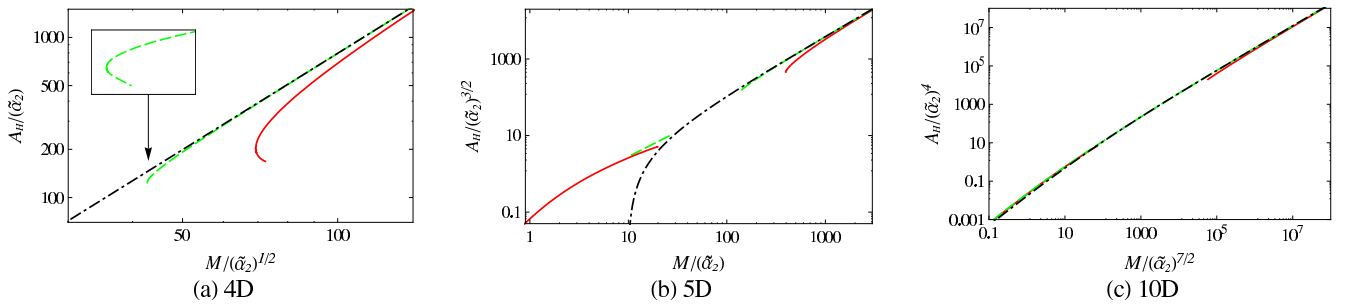


FIG. 10: The mass-area relations of black hole solutions in four dimensions, five dimensions, and ten dimensions. The dashed (green), dot-dashed (black), and solid (red) lines are the cases of the TDEGB, EGB, and DEGB models, respectively.

#### B. Thermodynamics

For the TDEGB model (2.7), the entropy is given by

$$S_T = \frac{A_H}{4} \left( 1 + \frac{2\tilde{\alpha}_2}{r_H^2} e^{-\gamma\phi_H} \right), \quad (8.1)$$

The corrections from the Bekenstein-Hawking entropy is

$$S_T - S_{\text{BH}} = \frac{2\tilde{\alpha}_2}{r_H^2} e^{-\gamma\phi_H} \times S_{\text{BH}} > 0. \quad (8.2)$$

This means that the entropy is always larger than the Bekenstein-Hawking's one in the TDEGB model as well. The

difference between (5.6) and (8.2) comes from the truncated term  $\mathcal{F}$  (note that the values of  $\phi_H$  in the DEGB theory and the truncated one are different).

Here, we show the black hole entropy and temperature in Figs. 11 and 12, respectively. In these figures, the solid (red) line, dashed (green) line, and dot-dashed (black) line describe the results for the DEGB, TDEGB, and EGB models, respectively.

The entropy behaves quite similarly to the area for all models, although the values are slightly different as shown in Fig. 2 in the DEGB model. There is no qualitative difference between  $A_H$  and  $S$ , except for  $D = 4$  in the TDEGB model for which we find a cusp near  $M \approx M_{\min}^{(\text{TDEGB})}$  instead of a turn-around smooth curve [21]. The cusp is related to a stability

change understood by a catastrophe theory [22].

As for the temperature, the behaviours are quite different in each model depending on the dimensions. In four dimensions, just as the area or the entropy, there appears a turning point, at which stability changes as we expected [20]. The same behaviour is found in the TDEGB model. In the EGB model, it is just a Schwarzschild black hole, i.e.,  $T_H \propto 1/M$ .

In five dimensions, however, there is a maximum temperature  $T_{\max} = 0.251938\tilde{\alpha}_2^{-1/2}$  at  $M = 15.0506\tilde{\alpha}_2$  in the DEGB model, just as in the EGB model ( $T_{\max} = \frac{\sqrt{6}}{8\pi}\tilde{\alpha}_2^{-1/2}$  at  $M = 4\pi^2\tilde{\alpha}_2$ ), although we have a mass gap. The temperature in the TDEGB model decreases monotonically as the mass increases.

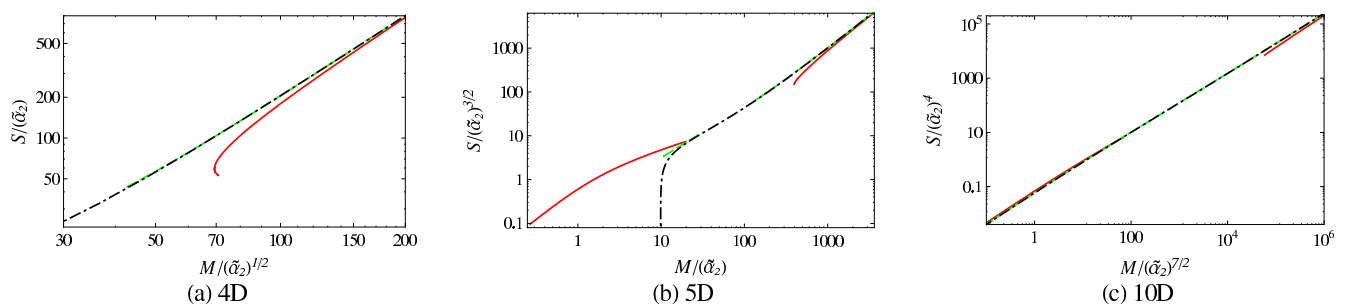


FIG. 11: The entropies of black holes with respect to the gravitational mass. The solid (red), dashed (green), and dot-dashed (black) lines are for the DEGB, TDEGB, and EGB models.

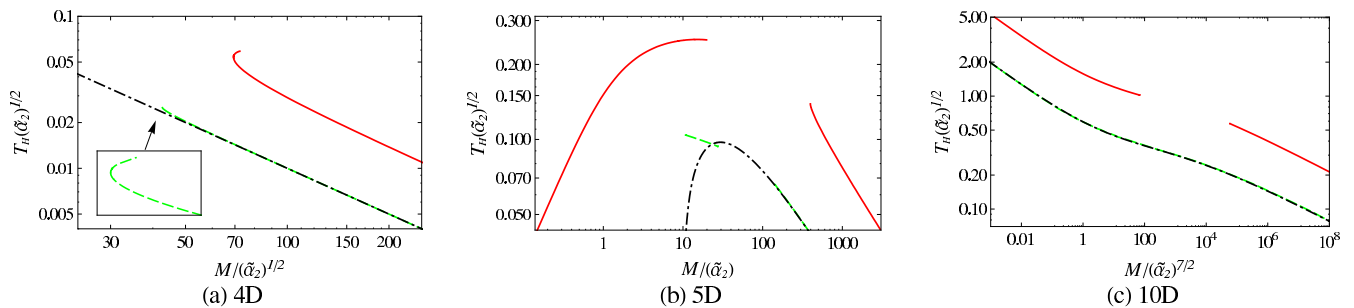


FIG. 12: The temperature of black holes with respect to the gravitational mass. The solid (red), dashed (green), and dot-dashed (black) lines are for the DEGB, TDEGB, and EGB models.

In ten dimensions, the temperature decreases monotonically with respect to the mass except near the turning point in the L-branch. There is no maximum temperature just as in the TDEGB and EGB models. In the L-branch of the DEGB model, however, we always find a turning point.

From this observation, we may conclude as follows: In four dimensions, both the DEGB and TDEGB models predict almost the same. When the black hole mass approaches the minimum value, the temperature is still finite. So the evaporation may not stop there. We suspect that either it evolves into a naked singularity, or it becomes time-dependent.

In five dimensions, however, two models give quite different predictions. In the DEGB model, in the zero-mass limit, we find that the temperature also vanishes. Then we expect that the black hole evaporate quietly. On the other hand, in the

TDEGB model, no black hole exists below the minimum mass  $M_{\min}^{(S)}$  and beyond the maximum temperature  $T_{\max}$ . When a black hole goes beyond this point via Hawking evaporation, we will find a naked singularity or a time-dependent black hole spacetime.

If the spacetime dimension is higher than five, two models will give the similar fate, i.e., a black hole evaporates violently because the temperature diverges in the mass-zero limit.

## IX. CONCLUDING REMARKS

We summarize our results in Table IV. The main difference in the DEGB model from the TDEGB model is that the exist-



tence of a turning point in five and higher dimensions and a zero-mass black hole in five dimensions. The Hawking temperature in the five-dimensional DEGB model vanishes at the zero-mass limit, but that in the TDEGB model is finite. The DEGB model also gives a maximum temperature in five dimensions. It may suggest that the DEGB model is better than the truncated one. In fact, the maximum temperature is given by  $T_{\max} \approx 0.251938\tilde{\alpha}_2^{-1/2} = 0.290913\alpha'^{-1/2}$  at  $M = 15.0506\tilde{\alpha}_2$ , which is naively consistent with the result given by the perturbative approach ( $T_{\max} \sim 0.1\alpha'^{-1/2}$ ) [10].

We also include the result in the case of  $\gamma = 1/2$  [16]. The result in that model is almost qualitatively similar to our TDEGB model except for the five dimensions. In five dimensions, the result is the same as the Schwarzschild black hole rather than that in our TDEGB or in the EGB model, although we do not know the reason.

In this paper we consider only the asymptotically flat

spacetime. The asymptotically nonflat spacetimes, however, are also important. The asymptotically anti-de Sitter spacetime is especially interesting in the context of anti-de Sitter/conformal field theory (AdS/CFT) correspondence. AdS/CFT correspondence is a widely-believed conjecture which suggests that there exists a duality between bulk gravity and boundary conformal theory. Taking account into some quantum effects, i.e., the higher curvature correction terms, one may examine a strong coupling region via AdS/CFT. It may provide another confirmation for the conjecture. The gravity duals of Gauss-Bonnet gravity with nontrivial dilaton field was studied in [23]. The asymptotically AdS spacetime in the TDEGB models were also analysed [24, 25]. Since we find some important difference between the DEGB and TDEGB models in this paper, it is also interesting to analyse the asymptotically nonflat spacetimes in the DEGB theory, which is under study.

TABLE IV: The comparison between the DEGB and TDEGB models with the EGB model and Schwarzschild black hole as references. In the four-dimensional TDEGB model, we find a cusp instead of a turn-around smooth curve.

$D$		DEGB	TDEGB	TDEGB( $\gamma = 1/2$ )	EGB	Schwarzschild
4	mass range	$M > M_{\min}$	$M > M_{\min}$	$M > M_{\min}$	Schwarzschild black hole	$M \geq 0$
	turning point	yes	“yes (cusp)”	no		no
	$T_{\max}$	finite	finite	finite		$\infty$
	$T_H$ at $M_{\min}$	finite	finite	finite		$\infty$
5	mass range	$M_{\max}^{(S)} > M \geq 0, M > M_{\min}^{(L)}$	$M_{\max}^{(S)} > M > M_{\min}^{(S)}, M > M_{\min}^{(L)}$	$M > M_{\min}$	$M > M_{\min}$	$M \geq 0$
	turning point	yes	no	no	no	no
	$T_{\max}$	finite	finite	$\infty$	finite	$\infty$
	$T_H$ at $M_{\min}$	zero	finite	$\infty$	zero	$\infty$
6~10	mass range	$M_{\max}^{(S)} > M \geq 0, M > M_{\min}^{(L)}$	$M \geq 0$	the same as our TDEGB ( $\gamma = \sqrt{2}/(D-2)$ )	$M \geq 0$	$M \geq 0$
	turning point	yes	no		no	no
	$T_{\max}$	$\infty$	$\infty$		$\infty$	$\infty$
	$T_H$ at $M_{\min}$	$\infty$	$\infty$		$\infty$	$\infty$

### Acknowledgments

N.O. would like to thank T. Torii for valuable discussions. This work was partially supported by the Grant-in-Aid for Scientific Research Fund of the JSPS (Nos.19540308 and 20540283) and for the Japan-U.K. Research Cooperative Program, and by the Waseda University Grants for Special Research Projects.

### Appendix A: Black hole in the Einstein-Gauss-Bonnet theory

In this appendix, we summarize the properties of a black hole in the Einstein Gauss-Bonnet theory. The action is

$$\mathcal{S}_{\text{EGB}} = \frac{1}{2\kappa_D^2} \int d^D x \sqrt{-g} \left( R + \alpha_2 R_{GB}^2 \right). \quad (\text{A1})$$

We find the field equations by setting the dilaton field  $\phi = 0$ , and can reduce them as

$$\left[ r^{D-3} (k - f(r)) + \alpha_2 (D-3)_4 r^{D-5} (k - f(r))^2 \right]' = 0, \\ \delta'(r) = 0. \quad (\text{A2})$$

In four dimensions, the Gauss-Bonnet term does not give any contribution to the solution. We have just a Schwarzschild black hole, i.e.,  $f(r) = k - 2\mu/r$ . For  $D \geq 5$ , we find two

branches of the solutions as follows:

$$f(r) = f_{\pm}(r)$$

$$:= k + \frac{r^2}{2(D-3)_4\alpha_2} \left( 1 \mp \sqrt{1 + \frac{8(D-3)_4\alpha_2\mu}{r^{D-1}}} \right),$$

$$\delta(r) = 0, \quad (\text{A3})$$

where  $\mu$  is an integration constant, which is related to the gravitational mass  $M$  as  $(D-2)A_{D-2}\mu = \kappa_D^2 M$ . The asymptotic behaviour or the weak coupling limit, i.e.,  $\tilde{\alpha}_2\mu/r^{D-1} \ll 1$ , gives

$$f_+(r) \rightarrow k - \left[ \frac{2\kappa_D^2}{(D-2)A_{D-2}} \right] \frac{M}{r^{D-3}},$$

$$f_-(r) \rightarrow k + \left[ \frac{2\kappa_D^2}{(D-2)A_{D-2}} \right] \frac{M}{r^{D-3}} + \frac{(D-2)r^2}{(D-4)\tilde{\alpha}_2}. \quad (\text{A4})$$

The former is an asymptotically flat spacetime, while the latter is an asymptotically anti-de Sitter spacetime [26]. The black hole mass in the asymptotically flat case is given by

$$\bar{M} := \kappa_D^2 M$$

$$= \frac{(D-2)A_{D-2}}{2} r_H^{D-3} \left[ 1 + \frac{2(D-4)\tilde{\alpha}_2}{(D-2)r_H^2} \right], \quad (\text{A5})$$

and the Hawking temperature is

$$T_H = \frac{[(D-2)_3r_H^2 + (D-4)_5\tilde{\alpha}_2]}{4\pi r_H [(D-2)r_H^2 + 2(D-4)\tilde{\alpha}_2]}. \quad (\text{A6})$$

The entropy is given by the Wald's formula as

$$S_{\text{EGB}} = \frac{A_H}{4} \left( 1 + \frac{2\tilde{\alpha}_2}{r_H^2} \right), \quad (\text{A7})$$

In four dimensions, it is just a Schwarzschild spacetime. There is nontrivial contribution in the entropy from the Gauss-Bonnet term. Then we find

$$M_{\min} = 0, \text{ and } S_{\min} = 2\pi\tilde{\alpha}_2, \quad (\text{A8})$$

at  $r_H = 0$ , when the temperature diverges ( $T_{\max} = \infty$ ).

In five dimensions, we find the black hole mass and the Hawking temperature as

$$M = \pi^2 (3r_H^2 + 2\tilde{\alpha}_2) \quad (\text{A9})$$

$$T_H = \frac{3r_H}{2\pi [3r_H^2 + 2\tilde{\alpha}_2]}. \quad (\text{A10})$$

Then we find

$$M_{\min} = 2\pi^2\tilde{\alpha}_2, \quad S_{\min} = 0, \quad T_{\min} = 0, \quad (\text{A11})$$

at  $r_H = 0$ . We also find the maximum temperature as

$$T_{\max} = \frac{\sqrt{6}}{8\pi} \tilde{\alpha}_2^{-1/2}, \quad (\text{A12})$$

at  $r_H = \sqrt{2\tilde{\alpha}_2/3}$  ( $M_{\max} = 4\pi^2\tilde{\alpha}_2$ ).

For dimensions higher than five, we find

$$M_{\min} = 0, \text{ and } S_{\min} = 0, \quad (\text{A13})$$

at  $r_H = 0$ , when the temperature diverges ( $T_{\max} = \infty$ ).

- 
- [1] M.B. Green, J.H. Schwarz and E. Witten, *Superstring Theory* (Cambridge Univ. Press, Cambridge, England 1987).; J. Polchinski, *String Theory* (Cambridge Univ. Press, Cambridge, England 1998).
- [2] R. R. Metsaev and A. A. Tseytlin, *Nucl. Phys. B* **293**, 385 (1987).
- [3] D. J. Gross and J. H. Sloan, *Nucl. Phys. B* **291**, 41 (1987); A. A. Tseytlin, *Nucl. Phys. B* **584**, 233 (2000) [arXiv:hep-th/0005072].
- [4] D. Lovelock, *J. Math. Phys.* **12**, 498 (1971); **13**, 874 (1972).
- [5] B. Zwiebach, *Phys. Lett. B* **156**, 315 (1985); B. Zumino, *Phys. Rep.* **137**, 109 (1986).
- [6] D. G. Boulware and S. Deser, *Phys. Rev. Lett.* **55**, 2656 (1985); J. T. Wheeler, *Nucl. Phys. B* **268**, 737 (1986); D. L. Wiltshire, *Phys. Lett. B* **169**, 36 (1986); R. G. Cai, *Phys. Rev. D* **65**, 084014 (2002) [arXiv:hep-th/0109133].
- [7] R. C. Myers and J. Z. Simon, *Phys. Rev. D* **38**, 2434 (1988); T. Torii and H. Maeda, *Phys. Rev. D* **71**, 124002 (2005) [arXiv:hep-th/0504127]; G. Giribet, J. Oliva and R. Troncoso, *JHEP* **0605** (2006) 007 [arXiv:hep-th/0603177]; R. G. Cai and N. Ohta, *Phys. Rev. D* **74**, 064001 (2006) [arXiv:hep-th/0604088];
- For reviews and references, see C. Garraffo and G. Giribet, *Mod. Phys. Lett. A* **23**, 1801 (2008) [arXiv:0805.3575 [gr-qc]]; C. Charmousis, *Lect. Notes Phys.* **769**, 299 (2009) [arXiv:0805.0568 [gr-qc]].
- [8] G. W. Gibbons and K. Maeda, *Nucl. Phys.* **B298**, 741 (1988).
- [9] D. Garfinkle, G. T. Horowitz, and A. Strominger, *Phys. Rev. D* **43**, 3140 (1991).
- [10] C.G. Callan, R.C. Myers, M.J. Perry, *Nucl. Phys.* **B311**, 673 (1989).
- [11] P. Kanti, N. E. Mavromatos, J. Rizos, K. Tamvakis and E. Winstanley, *Phys. Rev. D* **54**, 5049 (1996) [arXiv:hep-th/9511071].
- [12] S. O. Alexeyev and M. V. Pomazanov, *Phys. Rev. D* **55**, 2110 (1997) [arXiv:hep-th/9605106].
- [13] T. Torii, H. Yajima, K. Maeda, *Phys. Rev.* **D55**, 739 (1997) [arXiv:gr-qc/9606034].
- [14] C. M. Chen, D. V. Gal'tsov, D. G. Orlov *Phys. Rev.* **D75**, 084030 (2007) [arXiv:hep-th/0701004].
- [15] C. M. Chen, D. V. Gal'tsov, D. G. Orlov *Phys. Rev.* **D78**, 104013 (2008) [arXiv:0809.1720[hep-th]].
- [16] Z. K. Guo, N. Ohta and T. Torii, *Prog. Theor. Phys.* **120**, 581 (2008) [arXiv:0806.2481 [gr-qc]].
- [17] D. V. Gal'tsov and E. A. Davydov, *JETP Lett.* **89**, 102 (2009) [arXiv:0812.5103 [hep-th]].
- [18] This scalar field  $\phi$  does not give a proper kinetic term. Rescaling

it as  $\varphi = \sqrt{2}\kappa_D \phi$ ,  $\varphi$  has a proper kinetic term.

- [19] R. M. Wald, Phys. Rev. D **48**, R3427 (1993) [arXiv:gr-qc/9307038];  
V. Iyer and R. M. Wald, Phys. Rev. D **50**, 846 (1994) [arXiv:gr-qc/9403028].
- [20] J. Katz, I. Okamoto and O. Kaburaki, Class. Quant. Grav. **10**, 1323 (1993);  
R. Parentani, J. Katz and I. Okamoto, Class. Quant. Grav. **12**, 1663 (1995) [arXiv:gr-qc/9410015].
- [21] T. Torii and K. Maeda, Phys. Rev. D **58**, 084004 (1998)
- [22] K. Maeda, T. Tachizawa, T. Torii and T. Maki, Phys. Rev. Lett. **72**, 450 (1994) [arXiv:gr-qc/9310015];  
T. Torii, K. Maeda and T. Tachizawa, Phys. Rev. D **51**, 1510 (1995) [arXiv:gr-qc/9406013];  
T. Tachizawa, K. Maeda and T. Torii, Phys. Rev. D **51**, 4054 (1995) [arXiv:gr-qc/9410016].
- [23] R. G. Cai, Z. Y. Nie, N. Ohta, Y. W. Sun Phys. Rev. **D79**, 066004 (2009) [arXiv:0901.1421[hep-th]].
- [24] Z. K. Guo, N. Ohta and T. Torii, Prog. Theor. Phys. **121**, 253 (2009) [arXiv:0811.3068 [gr-qc]].
- [25] N. Ohta and T. Torii, Prog. Theor. Phys. **121**, 959 (2009) [arXiv:0902.4072 [hep-th]].
- [26] If  $\tilde{\alpha}_2 < 0$ , we find an asymptotically de Sitter spacetime.